Interpretation of Mono-Pulse Ice Radar Soundings on Two Peruvian Glaciers

KENNETH CHARLES JEZEK AND LONNIE G. THOMPSON

Abstract—During the 1979 and 1980 field seasons, mono-pulse radar sounding experiments were carried out on the Quelccaya Ice Cap in southern Peru and the col of Huascarán in northern Peru. Along with ice thickness determinations, some of which are described in detail elsewhere (the maximum ice thickness measured using the radar was 165 ± 20 m for the Quelccaya Ice Cap and 190 ± 10 m for Huascarán), studies were conducted to estimate the average temperature of the glaciers and the character of the glacier beds using the measured amplitudes and phases of the radar data. Values for the electrical properties of ice needed to model absorption in the ice reflection amplitudes at the ice base were compiled from the literature and extrapolated down to 5 MHz. An ambiguity in the interpretation of the radar data, regarding the relative contributions of reflection and absorption losses to the total attenuation, could only be resolved by including additional independent information about the glaciers such as 15-m temperatures and evidence for sliding around the perimeter. We conclude from these data that both the Quelccaya Ice Cap and the col of Huascarán are temperate glaciers which are dry-based near their summits and, in the case of Quelccaya, wet-based near the margin.

Manuscript received October 9, 1981; revised February 12, 1982. This work was supported by the National Science Foundation, Division of Atmospheric Sciences under Grant ATM 7821609 and the Division of Polar Programs under Grant GV 41411.

The authors are with the Institute for Polar Studies, Ohio State University, Columbus, OH 43210.

I. Introduction

A MONO-PULSE ice radar sounder has been used for ice thickness determinations on the Quelccaya Ice Cap (13°56′S, 70°50′W) in the Cordillera Oriental of southern Peru at an elevation of 5650 m and on the col of Huascarán (9°07′S, 77°36′W) in the Cordillera Blanca of northern Peru at an elevation of 6000 m. Ice thickness determinations (Fig. 1) for the Quelccaya Ice Cap are discussed by Thompson *et al.* [1]. Using an identical procedure, ice thicknesses have been calculated for Huascarán (Fig. 2). Ice thickness determinations, coupled with current accumulation rates, are used to estimate the length of the climatic record available from ice cores drilled to bedrock. Additionally, in northern Peru, which is located in an active earthquake zone, ice thickness determinations are important in calculating the volume of ice which might avalanche and, by calculating the amount of water likely to be displaced by an avalanche proceeding into a glacial lake, potential flood areas can be identified.

The data collected by Thompson in 1979 and 1980 on the Quelccaya Ice Cap and by Thompson in 1980 on the col of Huascarán included the relative amplitudes and phases of the reflected waves as well as travel-time measurements; therefore,

0196-2892/82/0700-0243$00.75

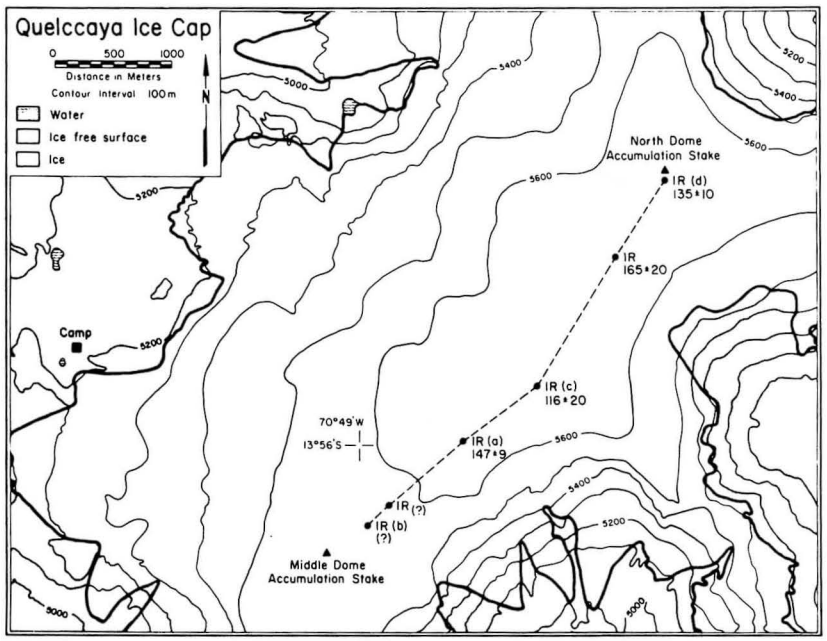

Fig. 1. Elevation contours and radar sounding sites on the Quelccaya Ice Cap. The numbers with error estimates (one standard deviation) are ice thicknesses in meters as determined by radar sounding. Question marks identify sounding sites where the bottom echo could not be identified. The lower case letters, a, b, c, and d correspond to sounding data presented in Fig. 3(a)–3(d).

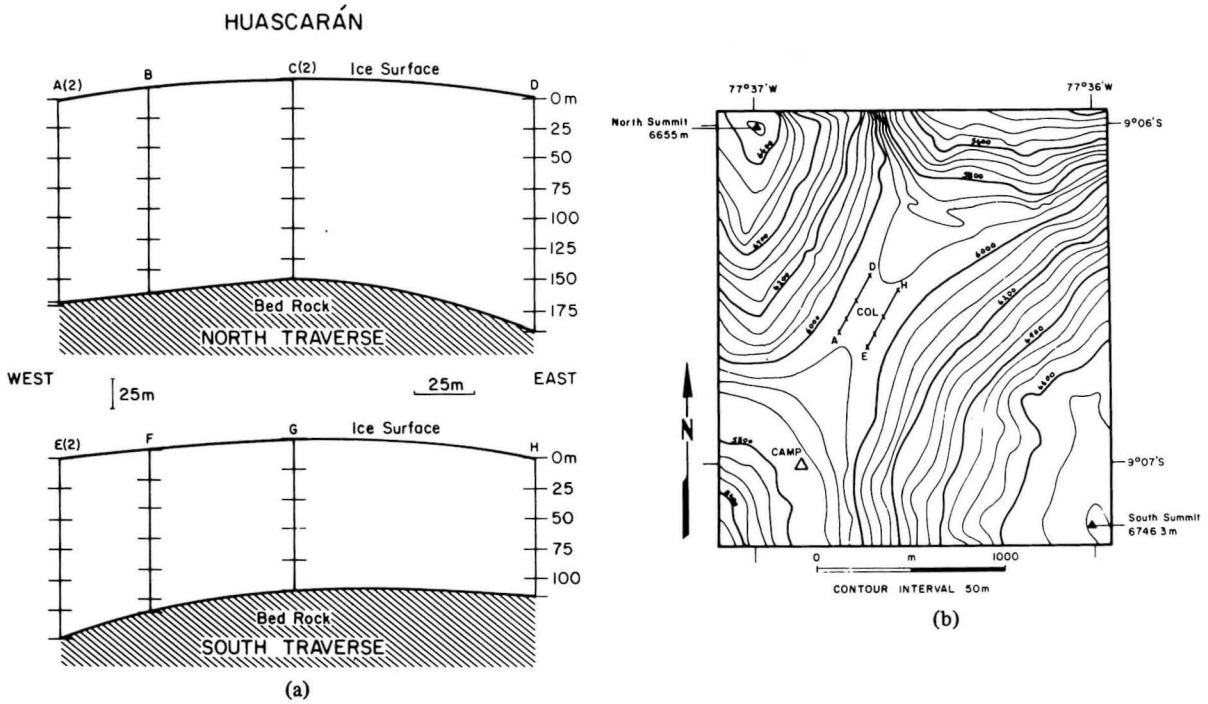

Fig. 2. (a) Ice thickness profiles on the col of Huascarán along two parallel lines which are shown in plan view in Fig. 2(b). (b) Elevation contours and radar sounding sites on the col of Huascarán.

we have investigated the internal composition of the ice masses, more closely focusing upon the average temperature within the ice cap and the nature of the ice bed. We have not been totally successful in resolving many of the ambiguities arising during the analysis; such as estimating a good value for the bottom reflection coefficient, however, these calculations will be of interest to others conducting similar investigations.

II. Mono-Pulse Ice Radar Sounder

The radar used on the Quelccaya Ice Cap and the col of Huascarán was designed to minimize scattering from pockets of water commonly found in temperate glaciers by ensuring that the wavelength of the radar wave is much greater than the predicted size of the scattering pockets [2], [3]. The design

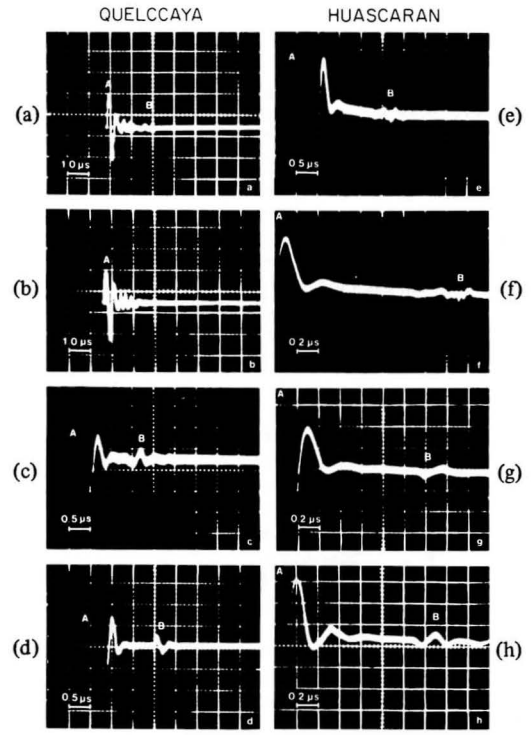

Fig. 3. Sample radar data from the Quelccaya Ice Cap and the col of Huascarán. The letter *A* identifies the surface wave which travels in air and the letter *B* identifies the reflection from the bottom of the ice. Complete wave forms are shown in Fig. 3(a) and 3(b) but a triggering malfunction resulted in the loss of the initial part of the surface wave in the remaining samples. The data presented in Fig. 3(e) and 3(f) were collected at the same location and demonstrate the complexity of the received waves on Huascarán and also that no arrivals are detected later than about 2 μs. The horizontal bar in the lower left-hand corner of each photo defines the time base. Waveforms (e) and (f) correspond to location *C*, (g) to location *H*, and (h) to location *F* in Fig. 2(a).

of the radar followed that of Vickers and Bollen, of the Stanford Research Institute under contract to the U.S. Geological Survey. The design was reported to us by Hodge (personal communication).

The equipment consists of a transmitter, used to generate voltage steps a few hundred volts in amplitude, and identical transmitting and receiving antennas. The antennas, resistively loaded dipoles tuned to radiate a single cycle at 5 MHz, were placed directly on the surface and separated by 50 to 100 m. Since signal levels were strong, the receiving antenna was coupled directly to an oscilloscope from which the data were recorded on Polaroid film. The oscilloscope time base, calibrated prior to going into the field, was used as the reference for all time measurements.

Examples of the data are shown in Fig. 3 and the locations of all sites where radar soundings were made are plotted in Figs. 1 and 2. The surface wave (*A* in Fig. 3(a)) excited in the upper medium (air), was used as a reference for travel-time, amplitude, and phase measurements. A triggering malfunction (described in Thompson and others, 1982) caused the loss of the initial parts of some of the surface waves resulting in some zero time uncertainty (Fig. 3(c)-(h)) and so we were forced to correlate latter parts of the surface wave with corresponding parts of the reflected wave. Bottom reflections on the Quelccaya Ice Cap (*B* in Fig. 3(a)) collected above the 5600-m elevation contour are strong and clean suggesting a smooth bottom while below 5600 m (Fig. 3(b)) the bottom reflection is obscured by what we believe to be scattering from an unusual amount of water in the ice [4]. The data collected on the col of Huascarán do not show arrivals from scatters above the ice-rock interface; however, the reflection from the ice-rock interface itself seems complicated, possibly due to bottom roughness.

III. Analysis

It has long been realized [5] that the absorption of electromagnetic waves in ice increases with temperature, thus providing a technique for estimating the average temperature within large ice bodies. Thus if the total attenuation of a transmitted wave is recorded and other sources of attenuation (reflection and scattering losses, geometrical losses) can be estimated, the portion of the total attenuation due to absorption can be found. Then, in principle, this value can be compared to predicted values of absorption at different temperatures and the average temperature in the ice can be deduced. In practice this procedure is complicated by uncertainties in the reflection properties of the ice bed, scattering losses within the ice, depolarization of the radar wave, and most importantly, uncertainty in the temperature dependence of absorption at different frequencies. The total attenuation, (A_t), measured as the ratio of the amplitudes of the surface wave and reflected wave, may be expressed as

$$A_t = A_b + G + S + R(\text{dB}) \tag{1}$$

where A_b is the absorption of the wave in ice, G is the geometrical loss, S is scattering loss in the ice, and R is the reflection coefficient. (Numerical values for these terms are summarized in Table I). S is assumed small because of the radar pulse wavelength ($\sim$ 34 m in ice) which was selected in view of the sizes of water pockets reported in temperate glaciers ($\lesssim$ 1 m) (this assumption is valid only in the central parts of the ice caps as described later).

A. Geometrical Losses

The received power of a dipole antenna is given by [6]

$$P_r = P_t \frac{g^2 \lambda^2}{4\pi r^2} \tag{2}$$

where g is the gain of the antenna, λ is the free-space wavelength, and r is the total travel path. For our amplitude reference we used the surface wave; the amplitude of which falls off as r^{-2} for a dielectric boundary [7], [8]. We have assumed that the other antenna parameters remain the same for both the wave transmitted into the ice and the surface wave and, therefore, the total geometrical effect becomes

$$G = \frac{P_I}{P_A} = \frac{r_a^4}{r_I^2} \tag{3}$$

where r_a is the separation between transmitting and receiving antennas and r_I is distance the wave travels in ice. Notice that these values are greater than one since the surface wave decays more rapidly than the wave transmitted into the ice; therefore, the magnitude of $(A_T - G)$ is increased.

TABLE I
SUMMARY OF THE PARAMETERS USED TO ESTIMATE THE AVERAGE TEMPERATURE OF THE QUELCCAYA ICE CAP AND THE COL OF HUASCARÁN

(Locations of sounding sites (L) are shown in Figs. 1 and 2. The ice thickness (IT) represents the total travel path rather than vertical thicknesses, AS is antenna separation. The errors associated with A_t (total attenuation), A_s (the absorption estimated for the upper 30 m of snow and firn, A_b (the absorption estimated for the solid ice), and G (the geometrical spreading loss) represent our best estimates of one standard deviation. R is the reflection coefficient at the ice–rock interface. The error for Quelccaya represents a statistical average of variations in ice thickness calculated from multiple records obtained from each location. Only one record was obtained for each location on Huascarán. We estimate a travel-time reading error of 0.05 μm · s which corresponds to an ice thickness uncertainty of about ±10 m.)

L	IT (m)	AS (m)	A_t (dB)	G (dB)	A (dB	R (dB)	A_b/thickness (dB/m)
				Quelccaya Ice Cap			
a	149±9	50	-24±2	19±1	-8±1	0	.147±.013
						-20	.063±.013
c	118±20	50	-18±2	21±1	-8±1	0	.176±.013
						-20	.063±.013
d	144±10	100	-24±2	31±1	-8±1	0	.206±.013
						-20	.118±.013
				Col of Huascarán			
A	164±10	50	-33±2	18±1	-8±1	0	.160±.013
						-20	.086±.013
C	123±10	50	-33±2	20±1	-8±1	0	.240±.013
						-20	.134±.013
D	192±10	50	-36±2	16±1	-8±1	0	.136±.013
						-20	.074±.013
E	144±10	50	-29±2	19±1	-8±1	0	.175±.013
						-20	.088±.013
F	130±10	50	-28±2	20±1	-8±1	0	.200±.013
						-20	.100±.013
H	139±10	50	-27±2	19±1	-8±1	0	.174±.013
						-20	.083±.013

B. Electromagnetic Absorption

The absorption of electromagnetic waves is determined by the electrical properties of ice which have been found to obey a Debye-type dispersion

$$\epsilon^* = \epsilon_\infty + \frac{\epsilon_s - \epsilon_\infty}{1 + i\omega\tau} \tag{4}$$

where ϵ^* is the complex permittivity, ϵ_∞ and ϵ_s are the high-frequency and static permittivities, τ is the dielectric relaxation time, and ω is the angular frequency [9]. We are unaware of measurements of ϵ^* conducted on ice at 5 MHz and, therefore, have used laboratory and field determinations of ϵ_s, ϵ_∞, and τ at higher frequencies and the Debye relation to estimate the properties of ice at 5 MHz.

For ice at radar frequencies, the real part of the permittivity ≈ 3.18, does not vary significantly with temperature for our purposes [10]. The loss tangent, equal to the quotient of the imaginary and real parts of (4), is

$$\tan\delta = \frac{\epsilon_s - \epsilon_\infty}{\epsilon_s + \epsilon_\infty \omega^2 \tau^2} \tag{5}$$

and is used to calculate absorption. In this equation ϵ_s and τ are functions of temperature and ϵ_s can be evaluated using the Curie-Weiss law

$$\epsilon_s = \frac{A_c}{T - T_c} + \epsilon_\infty \tag{6}$$

where A_c is a constant and T_c is the Curie temperature. Johari and Jones [11] report values of 23 400 and 15 K for A_c and T_c, respectively.

Westphal [12] has directly measured the loss tangent of glacial ice (collected on the Ward-Hunt Ice Shelf) at various temperatures and frequencies above 150 MHz. These values of tan δ are used to estimate τ as a function of temperature (5) and then to extrapolate Westphal's measurements down to 5 MHz. The calculated values of tan δ found using this technique are less than one and so we can express the attenuation, α, as

$$\alpha = 8.686 \frac{\pi f}{c} \sqrt{\epsilon'} \tan\delta \text{ (dB/m)}. \tag{7}$$

The variation of the attenuation with temperature deduced from Westphal's data is plotted in Fig. 4.

The dielectric relaxation time has been directly estimated by a number of authors using laboratory ice at various temperatures. Values of τ measured at 0°C are quoted in Table 2.3 of Hobbs [13] and these have been used to calculate a range of tan δ and α at 0°C (Fig. 4). Auty and Cole [14] report that the variation of τ with temperature for laboratory ice can be expressed as

$$\tau = C_\tau \exp\frac{E}{kT} \tag{8}$$

where C_τ is a constant equal to 5.3×10^{-16} s, E is the activation energy (.57 eV), k is Boltzmann's constant, and T is the temperature in degrees Kelvin. Inserting values of τ estimated

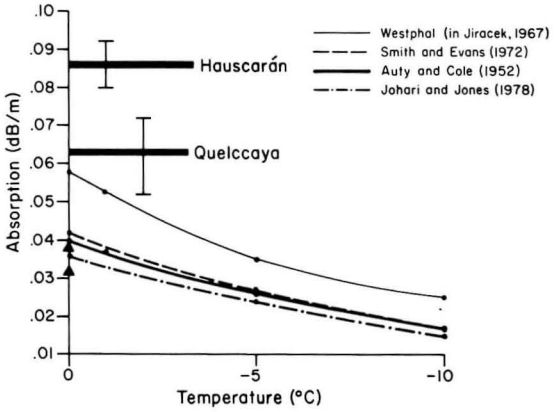

Fig. 4. The variation of α at 5 MHz with temperature and the attenuations calculated from the radar data. Curved lines are extrapolations of laboratory and field data down to 5 MHz: —Auty and Cole [14], -•-•- Johari and Jones [11], Smith, and Evans [2], --- Westphal [12]—. Triangles represent the attenuations calculated using the extreme values of τ at 0°C [22]. Horizontal lines represent the arithmetic means of the absorptions calculated from the radar data for each glacier and assuming a -20-dB reflection coefficient. Errors bars represent the standard deviation of the models. The arithmetic mean of the Huascarán data excludes the highest value because of the poor quality of that wave form. The mean of the Quelccaya data also excludes the highest value because the value corresponds to the unusual 0° phase shift datum.

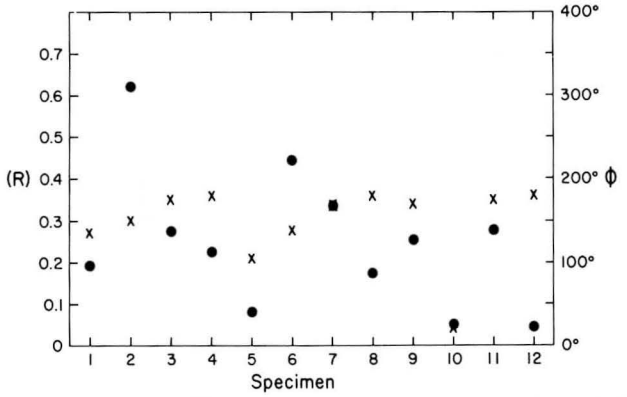

Fig. 5. Reflection coefficients (solid circles) and phases (crosses) for a two layer model involving ice and rock. The samples are 1) frozen sand [12]; 2) frozen silica and mud [12]; 3) sandstone [12]; 4) granite [12]; 5) quartz [12]; 6) gravel [12]; 7) lapilli tuff [15]; 8) Colorado tuff [15]; 9) white lapilli tuff [15]; 10) USBM tuff [15]; 11) green lapilli tuff [15]; 12) rhyolite tuff [15].

from this relation into the Debye equation, we can again determine α (Fig. 4).

Tan δ can also be calculated if the high-frequency conductivity (σ) can be estimated since

$$\tan \delta = \frac{\epsilon''}{\epsilon'} = \frac{\sigma}{\omega \epsilon_0 \epsilon'}. \tag{9}$$

Paren [17] finds that for temperate ice

$$\sigma = 4.6 \times 10^{-5} \exp -\left[\frac{E}{R}\left(\frac{1}{T} - \frac{1}{T_0}\right)\right] \Omega^{-1} \cdot m^{-1} \tag{10}$$

where the activation energy E is taken to be 55 kJ/mol and R is the gas constant. The attenuations estimated using this technique are plotted in Fig. 4.

The most recent, and probably most reliable, work on the electrical properties of ice has been done by Johari and Jones [11] on laboratory grown ice crystals. Their work is for various orientations of single crystals. As they find no measurable anisotropy in the electrical properties of ice, their estimates of τ_0 and E for the combined data at all polarizations are used to calculate τ

$$\tau = \left(\frac{\tau_0}{T}\right) \exp \frac{E}{RT} \tag{11}$$

where $\tau_0 = 0.93$ ps/K and $E = 51.1$ kJ/mol. The calculated absorptions based on this work are also plotted in Fig. 4.

The different estimates of absorption in ice as a function of temperature at 5 MHz show large discrepancies, especially between the laboratory ice and the ice collected *in situ*. This may be due to varying impurity levels in the ice: Westphal's samples were collected on an ice shelf and, therefore, were likely to contain higher impurity levels than the laboratory ice. We are not sure of the level of impurities in the Peruvian glaciers and so rather than excluding any of the data at this point we present this spectrum of results as indicative of the possible upper and lower bounds of the variation of absorption with temperature.

C. Reflection Coefficient

We have estimated the reflection coefficient at the ice bed by utilizing available information about local geology. Specifically, the rock underlying Huascarán glacier is granite while most of the rock surrounding the Quelccaya Ice Cap is ignimbrite, a rhyolitic, lithified tuff. We were unable to find any measurements of the electrical properties of ignimbrite but there have been a number of measurements on different types of tuff [15], [16]. Using values of the complex permittivity for tuff, granite, and other materials possibly found beneath the glacier we calculated the reflection coefficient based on a simple two-layer model

$$R = \frac{\sqrt{\epsilon_2^*} - \sqrt{\epsilon_1^*}}{\sqrt{\epsilon_2^*} + \sqrt{\epsilon_1^*}} \tag{12}$$

where ϵ^* are the complex permittivities of each medium and where we assume near normal incidence and a smooth reflecting surface. The amplitude and phase results (Fig. 5) indicate that for materials likely to be found beneath the two ice caps (granite, quartz, tuff) there is about 0.20-dB reflection loss and a 180-degree phase shift. For one particular specimen of tuff, the phase shift is near zero but with a much lower reflected amplitude. The phase of the reflected wave relative to the surface wave for most of the data on Quelccaya and all the measurable data on Huascarán was found to be phase shifted by about 180° in all but one case, Fig. 3(c), which seems to have experienced almost no phase shift. The single case of a near-zero phase shift was not satisfactorily explained by the two-layer model unless unsupported assumptions are made about the specific material at the base of the ice. Therefore, some additional calculations involving a three-layer model were done to see if a thin layer of air or water, substances likely to occur at the glacier's base, might modify the phase of the pulse more strongly than the variation in the

electrical properties of the underlying rock. Assuming the pulse length is much longer than the layer thickness and that the attenuation in the layer is small, the reflection coefficient is given by

$$R = \frac{R_{12} - R_{23}e^{i\Phi}}{1 + R_{12}R_{23}e^{i\Phi}} \tag{13}$$

where R_{12} is the reflection coefficient between layers 1 and 2, R_{23} is the reflection coefficient between layers 2 and 3, and $\Phi = kh$ where h is the layer thickness, and k is the wave number in the second medium. (Although the transmitted pulse will be composed of a spectrum of frequencies, we have assumed that the processes involved in the ice are not dispersive, a good approximation for the propagation of the wave in solid ice where tan δ is small but possibly a poor approximation at conducting boundaries). The magnitude and phase of the reflection coefficient for ice, varying thicknesses of glacial melt water and USBM tuff (sample 10 in Fig. 5) show that for thin layers of water (about 1 cm) the returned wave undergoes a very slight phase shift but the magnitude of R is only about -25 dB—only becoming large for unusually thick layers of water. Similar calculations for ice, water, and rhyolitic tuff revealed that the phase shift of the reflected wave never approached 0°. Air was also used for the second medium but we found unreasonable thicknesses were required for near zero phase shifts. Finally, a highly conducting water interface was assumed and found to produce strong though negative reflection coefficients [13]. In any case, if liquid water does exist at the base, and a small amount is forced into the pores of the rock then the electrical properties of the rock can be changed substantially (several orders of magnitude in conductivity for less than 1-percent change in water content [16]). Water in pore spaces increases both the conductivity and permittivity making the reflection coefficient strong and negative. Although some water has been observed to flow out from beneath Quelccaya, the rate seems to be dependent on daily meteorological variations suggesting that the water may be forming only peripherally.

Because of the uncertainty of the reflection coefficient calculations, we will investigate two models; the first takes R to be about 0 dB representing conductive meltwater at the base and, the second, representing a frozen base, takes R to be about -20 dB. Neither of these models involves materials which produce a positive phase and the only material we have found likely to do so, the USBM tuff, also has a very low reflection coefficient, -25 dB.

We apply one additional correction for the upper snow layers which attenuate the wave less than does solid ice. The conductivity of snow has been calculated by Glen and Paren [17] using Looyenga's mixing equation

$$\epsilon^{1/3} - 1 = v(\epsilon_I^{1/3} - 1) \tag{14}$$

where ϵ_I is the permittivity of ice, and v is the ratio of the density of snow to that of ice. The imaginary part can be used to find the conductivity of snow (σ_s)

$$\sigma_s = \sigma_i v(0.68 + .32v)^2 \Omega^{-1} \cdot m^{-1} \tag{15}$$

where σ_i is the conductivity of ice. We assume an average temperature of -2°C for the upper 30 m of snow and firn. (If the temperature is higher, then the total attenuation in the firn increases reducing the attenuation in the ice). For 60 m of total travel path, the attenuation in the snow (A_s) is about -8 dB, with an error which we estimate to be less than ±1 dB.

D. Results

Subtracting the geometrical loss, reflection loss, loss in snow, and scattering losses from the measured attenuation, we are left with the absorption in ice due to electrical losses. The absorption in dB/m is found using the thickness of solid ice at each location (Table I). Comparing the measured absorption in Table I with the calculated values in Fig. 4, we see that only the absorptions found using a -20-dB reflection coefficient approach the calculated data. In Fig. 4, we have plotted a horizontal bar corresponding to the arithmetic mean of the absorption data for each glacier. The bars correspond to the dry-based case only.

We point out that the calculated absorptions are likely to be high under the assumptions we made. That is, the magnitudes of the reflection coefficients of ice over rock may be low since we have not included scattering off a rough surface. (Gundmandsen [18] states that for roughness features on the order of $\lambda/2\pi$ scattering losses are about -4 dB). Also, there may be some attenuation due to scatterers in the ice. We are unable to quantitatively evaluate these uncertainties except to point out that the Quelccaya data do not show distorted reflections nor are there significant arrivals after the reflection we interpret as coming from bedrock—suggesting the base is smooth. On the other hand, the base at Huascarán may be very rough because it is in the col between two mountain peaks and the reflections are seen to be the combinations of many arrivals (Fig. 3(e) and 3(f)). It is, of course, possible that the local reflecting surface is smooth but the regional topography varies rapidly enough to cause multiple arrivals in a narrow time interval.

The results of both glaciers show considerable scatter. The estimated uncertainty in the absorption at each site is about ±3 dB corresponding to an average error in absorption of ±0.013 dB/m). Much of the variation between sites may be due to real changes in the reflection coefficient or, less likely, the temperature profile at each site. Assuming that the reflection coefficient and temperature profile are constant over the area of investigation and that the variations in absorption are indeed random, we have calculated the arithmetic mean and the standard deviation of the data for each model of R (Fig. 4). These models roughly indicate that the ice sheets temperatures are on average 0°C.

IV. Concluding Remarks

The results of the calculations on the radar data suggest that both ice caps are temperate throughout. Two of the results on Quelccaya fall statistically with the bands of predicted absorption for 0°C. The third value, corresponds to the 0° phase shift datum, can be brought near the band if a 27-dB reflection coefficient is assumed, corresponds to the USBM tuff. In any case, it seems likely that in the vicinity of the ice cap summit, the glacier is dry based.

All the data on Huascarán fall significantly higher than the predicted absorption. We know of no reason why absorption losses should be higher in Huascarán than Quelccaya and,

therefore, postulate that scattering losses from a rough surface are likely to be significant.

Our interpretation of average temperature within the glacier is supported by most of the other data collected on and around the Quelccaya Ice Cap. Temperature measurements on the summit of the ice cap and to a depth of 15 m show a warming to $\approx -0.5^{\circ}$C with depth. Above the 5600-m elevation contour, radar data indicate little free water (based on the absences of internal scatters) in the body of the glacier and also indicate a dry bed. This observation is supported by associated oxygen isotope records which are well preserved with depth and thus imply that there is little if any free water percolating down into the glacier [19]. However, below the 5600-m elevation contour the radar data become confused with internal scatterers and the oxygen isotope records are smoothed suggesting the presence of free water in the body of the glacier. Also, ice caves found around the perimeter of the ice cap indicate that at least in these areas the glacier is sliding and therefore the basal temperatures are near the pressure melting point. The radar data collected near the margin of the glacier show a number of echos which obscure the ice rock reflection, a characteristic of temperate glaciers containing water pockets.

We have less information about Huascarán to help us deduce its thermal regime and thermal history. Although Huascarán is ≈600 m higher than Quelccaya, it is 5° closer to the equator so it is unlikely that the local environments of the two glaciers are distinctively different now or have been in the past. We conclude that Huascarán is also temperate and probably dry based but that its bed is significantly rougher than Quelccaya. In view of the characteristics of the radar data, we further suggest that the percentage of free water in the Huascarán glacier is similar to that in the highest elevations of the Quelccaya Ice Cap.

Acknowledgment

The authors gratefully acknowledge the Peruvian Instituto Geológico Minero y Metalurgico for field and logistical support. We would especially like to thank E. Mosley-Thompson, J. Bolzan, and I. Whillans for reviewing this manuscript. We also wish to thank J. Cothran for typing this paper.

References

[1] L. G. Thompson, J. F. Bolzan, H. H. Brecher, P. D. Kruss, E. Mosley-Thompson, and K. C. Jezek, "Geophysical investigations of the tropical Quelccaya Ice Cap," submitted to *J. Glaciology*, vol. 28, no. 98, 1982.

[2] B. M. Smith and S. Evans, "Radio echo sounding: Absorption and scattering by water inclusion and ice lenses," *J. Glaciology*, vol. 17, no. 75, pp. 133-146, 1972.

[3] R. D. Watts and A. W. England, "Radio echo sounding of temperate glaciers: Ice properties and sounder design criteria," *J. Glaciology*, vol. 17, no. 75, pp. 39-45, 1976.

[4] R. D. Watts and W. Isherwood, "Gravity surveys in glacier-covered regions," *Geophysics*, vol. 43, no. 4, pp. 819-822, June 1978.

[5] R. G. de Q, S. Evans, and J. T. Bailey, "Interpretation of radio echo sounding in polar ice sheets," *Philosophical Trans. Royal Society of London*, Serv. A, vol. 265, no. 1166, pp. 437-505, Dec. 1969.

[6] *Reference Data for Radio Engineers*, H. P. Westman, Ed. New York: Howard W. Sams and Co., Inc., 1969, pp. 25-28.

[7] K. C. Jezek, J. W. Clough, C. R. Bentley, and S. Shabtaie, "Dielectric permittivity of glacier ice measured *in situ* by radar wide-angle reflection," *J. Glaciology*, vol. 21, no. 85, pp. 315-329, 1978.

[8] J. R. Wait, "Theory of ground wave propagation," in *Electromagnetic Probing in Geophysics*, J. R. Wait, Ed., Boulder, CO: Golem Press, 1971, pp. 163-207.

[9] P. V. Hobbs, *Ice Physics*. Oxford, England: Clarendon Press, 1974, p. 84.

[10] G. P. Johari and P. A. Charette, "The permittivity and attenuation in polycrystalline and single-crystal ice Ih at 35 and 50 MHz," *J. Glaciology*, vol. 14, no. 71, pp. 293-303, 1975.

[11] G. P. Johari and S. J. Jones, "The orientation polarization in hexagonal ice parallel and perpendicular to the c-axis," *J. Glaciology*, vol. 21, no. 85, pp. 259-276, 1978.

[12] G. P. Jiracek, "Radio sounding of Antarctic ice," University of Wisconsin, Geophysical Land Polar Research Center, Research Report Series, 67-1, 1967.

[13] P. V. Hobbs, *Ice Physics*. Oxford, England: Clarendon Press, 1974, p. 93.

[14] R. P. Auty and R. H. Cole, "Dielectric properties of ice and solid D_2O," *J. Chemical Physics*, vol. 20, pp. 1309-1314, 1952.

[15] G. R. Olhoeft, Tables of room temperature electrical properties for selected rocks and minerals with dielectric permittivity statics, US Geological Survey, Denver, CO, Open file Report 79-993, 1979.

[16] E. I. Parkhomenko, *Electrical Properties of Rocks*. New York: Plenum Press, 1967.

[17] J. W. Glen and J. G. Paren, "The electrical properties of snow and ice," *J. Glaciology*, vol. 15, no. 73, pp. 15-38, 1975.

[18] P. Gudmandsen, "Electromagnetic probing of ice," in *Electromagnetic Probing in Geophysics*, J. R. Wait, Ed., Boulder, CO: Golem Press, 1971, pp. 321-348.

[19] L. G. Thompson, "Glaciological investigations of the tropical Quelccaya Ice Cap, Peru," *J. Glaciology*, vol. 25, no. 91, pp. 69-84, 1980.

*

Kenneth Charles Jezek received the B.S. degree in physics from the University of Illinois, Urbana in 1973. He did graduate work in geophysics at the University of Wisconsin-Madison and received the Ph.D. degree in 1980 for work on the Ross Ice Shelf, Antarctica.

His current research interests center on the application of radar techniques to problems involving glacial dynamics and glacial history. He currently holds the position of Project Associate at the Geophysical and Polar Research Center of the University of Wisconsin-Madison.

*

Lonnie G. Thompson was born in Gassaway, WV. He received the B.S. degree in 1970 from Marshall University, Huntington, WV, and the M.S. and Ph.D. degrees in geology from The Ohio State University, Columbus, Ohio, in 1973, and 1976, respectively.

He is a Senior Research Associate of the Institute of Polar Studies, The Ohio State University. He has been engaged in the development and execution of glaciological research programs in both polar and high altitude regions for the past nine years. The primary emphasis of these research programs have been paleoclimatic reconstruction from ice cores drilled in polar ice sheets and alpine ice caps. He has been actively engaged in developing and perfecting the analytical procedures employed in the rapid measurement of particulate concentrations and size distributions in ice core samples. Since 1976, he has also been engaged in the study of tropical alpine glaciers where he has been applying ice core paleoclimatic reconstruction techniques. He has authored or co-authored over 20 papers on the subjects of microparticle ice core records from polar and tropical regions and their paleoclimatic importance. It is his involvement with tropical galciers and the need for accurately assessing their thickness that generated his interest in techniques for ice thickness determinations on temperate glaciers.

Dr. Thompson is a member of the International Glaciological Society, the American Geophysical Union, ANQUA, and the American Polar Society.